Inorganic Chemistry
Article

Inorg. Chem. **2010**, *49*, 2975–2982 **2975**
DOI: 10.1021/ic902504y

Systematic Study of Modifications to Ruthenium(II) Polypyridine Dyads for Electron Injection Enhancement

Elena Jakubikova, Richard L. Martin, and Enrique R. Batista*

Theoretical Division, Los Alamos National Laboratory, MS-B268, Los Alamos, New Mexico 87545

Received December 16, 2009

Spatial localization of excited-state electrons in transition-metal complexes used as photocatalysts or dye sensitizers in solar cells is important for efficient electron injection into the metal oxide nanoparticles. We use density functional theory to investigate the excited states in a prototype catalyst−chromophore assembly $[(bpy)(H_2O)Ru(tpy-tpy)Ru(tpy)]^{4+}$ ($[Ru(tpy)(bpy)(H_2O)]^{2+}$ = catalyst, $[Ru(tpy)_2]^{2+}$ = chromophore, tpy = 2,2′:6′,2″-terpyridine, and bpy = 2,2′-bipyridine) and a series of related compounds. We explore several bridging ligand and terminal tpy ligand modifications of the prototype assembly, with the aim of inducing electronic excitations into the terminal tpy ligand upon irradiation with visible light. The excitations into the terminal ligand (i.e., ligand covalently attached to the semiconductor in the photocatalytic synthetic cell) should, in turn, enhance electron injection into the semiconductor. Our results suggest that both introduction of a spacer group (such as phenylene or alkane) into the tpy−tpy bridge and replacement of the terminal tpy group by a more extended π-conjugated ligand are necessary to shift the electronic excitations from the bridging ligand into the terminal ligand. These results have implications for the design of photocatalysts and dye-sensitizer assemblies based on ruthenium(II) terpyridine compounds.

Introduction

Transition-metal complexes, ruthenium polypyridyl complexes in particular, are widely used as dyes in dye-sensitized solar cells[1] and as catalysts or photocatalysts capable of performing water oxidation[2−5] or oxidation of organic compounds.[6−11] They can also be used as chromophores to harvest solar energy because of their absorption in the visible-light region. Therefore, understanding the nature of the electronic excited states in transition-metal complexes is crucially important for elucidation of the mechanistic details of the photocatalyst function and the design of efficient molecular devices for solar energy conversion.

An important aspect of the molecular photocatalyst functionality is its ability to inject electrons into a metal oxide nanoparticle in order to induce charge separation and thus mimic photosynthetic charge-transfer events.[12−14] This is usually achieved by an excitation into a metal-to-ligand charge-transfer (MLCT) state that couples to the states in the nanoparticle conduction band, which leads to interfacial electron transfer (IET). IET competes with other processes that occur upon photoexcitation, such as radiative or nonradiative transition back to the ground state or intersystem crossing (IC) into the lowest triplet excited state. IC plays an important role in the case of the ruthenium polypyridyl complexes,[15] and the excited states that lead to electron injection into the semiconductor are a combination of initially populated singlet excited states and a thermalized ^{3}MLCT state.[16]

Previously, we reported IET dynamics in $[Ru(tpy)_2]^{2+}$ and $[(bpy)(H_2O)Ru(tpy-tpy)Ru(tpy)]^{4+}$ ($[Ru(tpy)(bpy)(H_2O)]^{2+}$ = model catalyst, $[Ru(tpy)_2]^{2+}$ = chromophore, tpy = 2,2′:6′,2″-terpyridine, and bpy = 2,2′-bipyridine) attached to an anatase TiO_2 nanoparticle via a phosphonic acid

*To whom correspondence should be addressed. E-mail: erb@lanl.gov.

(1) Ardo, S.; Meyer, G. J. *Chem. Soc. Rev.* **2009**, *38*, 115–164.
(2) Geselowitz, D.; Meyer, T. J. *Inorg. Chem.* **1990**, *29*, 3894–3896.
(3) Muckerman, J. T.; Polyansky, D. E.; Wada, T.; Tanaka, K.; Fujita, E. *Inorg. Chem.* **2008**, *47*, 1787–1802.
(4) Wada, T.; Tsuge, K.; Tanaka, K. *Angew. Chem., Int. Ed.* **2000**, *39*, 1479.
(5) Hurst, J. K. *Coord. Chem. Rev.* **2005**, *249*, 313–328.
(6) Thompson, M. S.; Meyer, T. J. *J. Am. Chem. Soc.* **1982**, *104*, 5070–5076.
(7) Thompson, M. S.; Degiovani, W. F.; Moyer, B. A.; Meyer, T. J. *J. Org. Chem.* **1984**, *49*, 4972–4977.
(8) Farrer, B. T.; Thorp, H. H. *Inorg. Chem.* **1999**, *38*, 2497–2502.
(9) Moyer, B. A.; Thompson, M. S.; Meyer, T. J. *J. Am. Chem. Soc.* **1980**, *102*, 2310–2312.
(10) Treadway, J. A.; Moss, J. A.; Meyer, T. J. *Inorg. Chem.* **1999**, *38*, 4386–4387.
(11) Chen, W.; Rein, F. N.; Rocha, R. C. *Angew. Chem., Int. Ed.* **2009**, *48*, 9672–9675.
(12) Sun, L. C.; Hammarstrom, L.; Akermark, B.; Styring, S. *Chem. Soc. Rev.* **2001**, *30*, 36–49.
(13) Falkenstrom, M.; Johansson, O.; Hammarstrom, L. *Inorg. Chim. Acta* **2007**, *360*, 741–750.
(14) Ghanem, R.; Xu, Y. H.; Pan, J.; Hoffmann, T.; Andersson, J.; Polivka, T.; Pascher, T.; Styring, S.; Sun, L. C.; Sundstrom, V. *Inorg. Chem.* **2002**, *41*, 6258–6266.
(15) Sauvage, J. P.; Collin, J. P.; Chambron, J. C.; Guillerez, S.; Coudret, C.; Balzani, V.; Barigelletti, F.; Decola, L.; Flamigni, L. *Chem. Rev.* **1994**, *94*, 993–1019.
(16) She, C.; Guo, J.; Irle, S.; Morokuma, K.; Mohler, D. L.; Zabri, H.; Odobel, F.; Youm, K.-T.; Liu, F.; Hupp, J. T.; Lian, T. *J. Phys. Chem. A* **2007**, *111*, 6832–6842.

Published on Web 02/08/2010

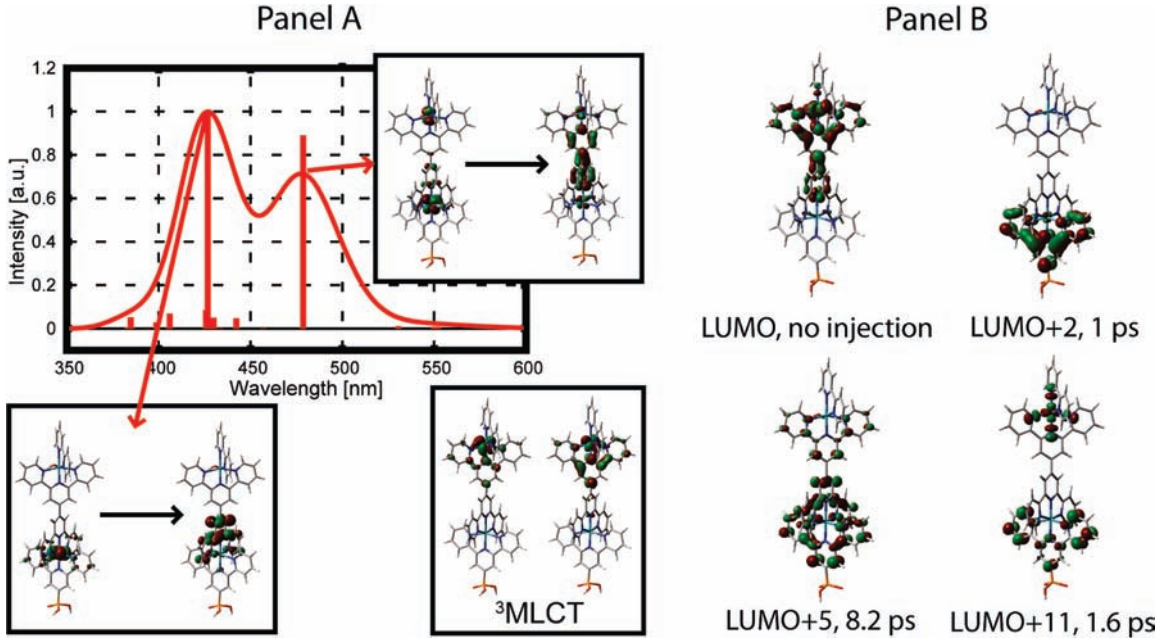

Figure 1. (A) Calculated absorption spectrum of $[(bpy)(H_2O)Ru(tpy-tpy)Ru(tpy(PO_3H_2))]^{4+}$ with NTOs for the most intense transitions and singly occupied natural orbitals of the optimized ^{3}MLCT state for the same molecule. (B) Selected virtual molecular orbitals of the $[Ru(tpy)(bpy)(H_2O)Ru(tpy)(tpy(PO_3H))]^{4+}$ adsorbate obtained from extended Hückel theory and their IET rates. Note that while IET occurs only from the orbitals localized on the terminal tpy(PO_3H_2) ligand, the most intense transitions, as well as the long-lived ^{3}MLCT state, are characterized by excited electron localization on the bridge. Taken from ref 17.

linker.[17] In that study, we found that while IET due to the visible-light photoexcitation of $[Ru(tpy)_2]^{2+}$ takes 1−10 ps, IET from $[(bpy)(H_2O)Ru(tpy-tpy)Ru(tpy)]^{4+}$ is much slower because the electronic excitation remains localized on the tpy−tpy bridge, which is weakly coupled to the conduction band of TiO_2 (see Figure 1).

Strictly speaking, the initial MLCT excited state does not need to be localized on the ligand directly attached to the semiconductor for IET to take place.[18−21] Electron injection from remote ligands is, however, less efficient and slower compared to injection from the ligands adjacent to the nanoparticle,[19,21] and it can take place via the electron−phonon coupling mechanism. Additionally, documented cases of IET from the excited state localized on the bridging ligand between two Ru metal centers employed $Ru(bpy)_3$-based dyads.[10,21] Because the excited-state lifetime of ruthenium(II) bis(terpyridine)-based dyads is an order of magnitude shorter than that of the $Ru(bpy)_3$-based dyads (∼100 ns for the former versus ∼1000 ns for the latter),[22] the tpy−tpy localized excited state might not live long enough for coupling to a more favorable state via phonons to take place. Moreover, IET from this ligand would be less efficient because of competition with other excited-state decay processes.[21] Therefore, here we explore a series of modifications to the bridging tpy−tpy and terminal tpy ligands in order to find variations of the previously studied molecule that would favor electronic excitations into the terminal tpy ligand with strong electronic coupling to the semiconductor. On the basis of these studies, a new dyad is proposed that balances the electron affinity of the bridging group versus the terminal group and captures the excitation next to the attachment group that links to the surface.

Methodology

All dyads were optimized in their singlet ground state at the B3LYP[23,24] level of theory using the LANL08 relativistic effective core potential and basis set[25,26] to describe the Ru center and the 6-31G* basis set[27,28] for all other atoms. Minimum-energy configurations of all dimers in their lowest triplet states were obtained at the same level of theory. The character of the unpaired spin density was determined from natural orbital analysis.[29] The *Gaussian 03* program[30] was used to perform all calculations.

(17) Jakubikova, E.; Snoeberger, R. C., III; Batista, V. S.; Martin, R. L.; Batista, E. R. *J. Phys. Chem. A* **2009**, *113*, 12532–12540.
(18) Liu, F.; Meyer, G. J. *Inorg. Chem.* **2005**, *44*, 9305–9313.
(19) Bonhote, P.; Moser, J. E.; Humphry-Baker, R.; Vlachopoulos, N.; Zakeeruddin, S. M.; Walder, L.; Gratzel, M. *J. Am. Chem. Soc.* **1999**, *121*, 1324–1336.
(20) Argazzi, R.; Bignozzi, C. A.; Heimer, T. A.; Meyer, G. J. *Inorg. Chem.* **1997**, *36*, 2–3.
(21) Gholamkhass, B.; Koike, K.; Negishi, N.; Hori, H.; Sano, T.; Takeuchi, K. *Inorg. Chem.* **2003**, *42*, 2919–2932.
(22) Harriman, A.; Ziessel, R. *Chem. Commun.* **1996**, 1707.
(23) Becke, A. D. *J. Chem. Phys.* **1993**, *98*, 5648–5652.
(24) Stephens, P. J.; Devlin, F. J.; Chabalowski, C. F.; Frisch, M. J. *J. Phys. Chem.* **1994**, *98*, 11623–11627.
(25) Hay, P. J.; Wadt, W. R. *J. Chem. Phys.* **1985**, *82*, 270–283.
(26) Roy, L. A.; Hay, P. J.; Martin, R. L. *J. Chem. Theory Comput.* **2008**, *4*, 1029–1031.
(27) Harihara, P. C.; Pople, J. A. *Theor. Chim. Acta* **1973**, *28*, 213–222.
(28) Hehre, W. J.; Ditchfield, R.; Pople, J. A. *J. Chem. Phys.* **1972**, *56*, 2257–2261.
(29) Davidson, E. R. *Rev. Mod. Phys.* **1972**, *44*, 451.
(30) Frisch, M. J.; Trucks, G. W.; Schlegel, H. B.; Scuseria, G. E.; Robb, M. A.; Cheeseman, J. R.; Montgomery, J. A.; Vreven, J. T.; Kudin, K. N.; Burant, J. C.; Millam, J. M.; Iyengar, S. S.; Tomasi, J.; Barone, V.; Mennucci, B.; Cossi, M.; Scalmani, G.; Rega, N.; Petersson, G. A.; Nakatsuji, H.; Hada, M.; Ehara, M.; Toyota, K.; Fukuda, R.; Hasegawa, J.; Ishida, M.; Nakajima, T.; Honda, Y.; Kitao, O.; Nakai, H.; Klene, M.; Li, X.; Knox, J. E.; Hratchian, H. P.; Cross, J. B.; Bakken, V.; Adamo, C.; Jaramillo, J.; Gomperts, R.; Stratmann, R. E.; Yazyev, O.; Austin, A. J.; Cammi, R.; Pomelli, C.; Ochterski, J. W.; Ayala, P. Y.; Morokuma, K.; Voth, G. A.; Salvador, P.; Dannenberg, J. J.; Zakrzewski, V. G.; Dapprich, S.; Daniels, A. D.; Strain, M. C.; Farkas, O.; Malick, D. K.; Rabuck, A. D.; Raghavachari, K.; Foresman, J. B.; Ortiz, J. V.; Cui, Q.; Baboul, A. G.; Clifford, S.; Cioslowski, J.; Stefanov, B. B.; Liu, G.; Liashenko, A.; Piskorz, P.; Komaromi, I.; Martin, R. L.; Fox, D. J.; Keith, T.; Al-Laham, M. A.; Peng, C. Y.; Nanayakkara, A.; Challacombe, M.; Gill, P. M. W.; Johnson, B.; Chen, W.; Wong, M. W.; Gonzalez, C.; Pople, J. A. *Gaussian 03*, revision E.01; Gaussian, Inc.: Wallingford, CT, 2004.

Time-dependent density functional theory (TD-DFT) calculations[31−33] were performed on selected ruthenium(II) polypyridine complexes in the visible-light region (approximately 400−700 nm). We used the B3LYP functional for the TD-DFT calculations on ruthenium polypyridyl monomers previously[34] and found an overall satisfactory agreement with the experiment, with the error between the experimentally measured and calculated maxima ranging from 0.16 to 0.37 eV. Recently, Chen et al.[11] published the visible absorption spectrum of $[Ru(tpy)(bpy)(H_2O)Ru(tpy)_2]^{4+}$ (dyad **A**), characterized by a strong absorption peak at ∼524 nm (2.37 eV) and a shoulder at ∼490 nm (2.53 eV). This compares well with the absorption peaks obtained by a B3LYP TD-DFT calculation at 2.45 and 2.76 eV, suggesting that the errors in our calculated visible absorption spectra for dimers will be similar to those observed in our previous work with the ruthenium polypyridyl monomers.[34]

Another important consideration for the accuracy of our calculations is the influence of the solvent effects on the calculated geometries and absorption spectra. All calculations presented here were performed in vacuo. As we discussed previously,[34] inclusion of the solvent effects via the polarizable continuum model (PCM) has only a minimal influence on the ground-state optimized geometries of the ruthenium polypyridyl compounds. It can be, however, important for the lowest triplet excited-state optimizations because a ^{3}MC (metal-centered) state, rather than the ^{3}MLCT state, is favored when a solvent is not included in the optimizations. This problem was addressed by including the first solvation shell explicitly (i.e., two H_2O molecules weakly bound to the H_2O ligand), in case the geometry optimization of the lowest triplet excited state in vacuo led to a ^{3}MC localized state (this was done for dyads **E**, **L**, and **Q**). As for the calculated absorption spectra, the inclusion of the solvent effects via the PCM results in a shift of less than 0.03 eV in the absorption peak maxima and in a relatively small increase of the peak intensities (see Figure S1 in the Supporting Information). Because inclusion of the solvent effects does not influence the calculated absorption spectra significantly, all TD-DFT calculations were performed in vacuo to avoid the added computational cost.

Natural transition orbital (NTO) analysis[35] was carried out to better understand the results of TD-DFT calculations. The NTO analysis was applied to transitions with calculated oscillator strength $f \geq 0.02$. Absorption spectra were simulated by convoluting the spectrum, composed of the δ functions at the excitation energies times the oscillator strengths, with a Lorentzian line shape. We set the half-width at half-maximum (hwhm) equal to 0.12 eV, which falls within the interval of the experimentally observed standard spectroscopic line widths for ruthenium polypyridyl compounds.[34] The resulting spectra were scaled by a factor of $1/4.33 \times 10^9$ to obtain the intensities measured in the molar extinction coefficient ε.[36]

Results and Discussion

The goal of this work is to determine how different modifications of the model catalyst−chromophore dyad (catalyst = $[Ru(tpy)(bpy)(H_2O)]^{2+}$; chromophore = $[Ru(tpy)_2]^{2+}$) influence the relative energies of the molecular orbitals located on the bridging ligand versus the molecular orbitals located on the terminal ligand of the chromophore. These energies will determine which of these molecular orbitals will be occupied by the excited electron, which is, in turn, important for an efficient electron injection into the semiconductor. The $[(bpy)(H_2O)Ru(tpy-tpy)Ru(tpy)]^{4+}$ dyad (dyad **A**) is taken as a starting point for all proposed modifications. For comparison, we also look at three dyads with chromophore subunits based on $[Ru(bpy)_3]^{2+}$.

We focus on two different properties: First, we determine the order of the lowest-energy virtual orbitals located on the bridge and terminal tpy or bpy ligand of the chromophore, as well as the energy gap between them. The ordering of these orbitals provides us, to a first approximation, with information about which ligand will reduce more readily upon photoexcitation. Second, we look at the electron localization in the lowest triplet excited state. This is achieved by geometry optimization of the lowest triplet excited state for all of the dimers. Finally, absorption spectra are obtained for selected dimers.

Modifications to the Bridging Ligand. To evaluate the influence of different groups on the relative stabilities of the bridging ligand and the terminal tpy/bpy group of the chromophore, we have tested nine bridging ligands connecting the model catalyst based on $[Ru(tpy)(bpy)(H_2O)]^{2+}$ to the chromophore based on $[Ru(tpy)_2]^{2+}$ or $[Ru(bpy)_3]^{2+}$. The bridging ligands chosen in this work were used in previous experimental studies for connecting various ruthenium polypyridyl compounds.[10,37−42] All of the dyads considered in this work are shown in Figure 2.

Figure 3 shows the energies, relative to the energy of the highest occupied molecular orbital (HOMO), of the lowest-energy virtual orbitals localized on the bridging ligand and the terminal tpy or bpy ligand of the chromophore subunit. The largest energy gap between the two levels and the greatest stabilization of the virtual orbitals localized on the bridging ligand is observed for the most strongly coupled catalyst−chromophore dyads containing 2,2′-bipyriminide (**I**) and tetrapyrido(2,3-*a*:3′,2′-*c*:2″,3″-*h*,3‴,2‴-*j*)phenazine (**D**) ligands because the π state located on the bridge is stabilized by the large π conjugation. The smallest gap is observed for bridging ligands in which conjugation of the tpy−tpy or tpy−bpy groups is broken by the insertion of additional groups, such as a phenylene spacer (**E**) or a 2,5-thiophenedyil spacer (**F**). Even in the case of the phenylene spacer, the gap between the two energy levels is rather high, approximately 0.6 eV. In all of the considered dyads, the lowest unoccupied molecular orbital (LUMO) is localized on the bridging ligand and the unpaired electrons in the lowest triplet excited state localize on the d orbital of ruthenium and the π^* orbital of the catalyst−chromophore bridging ligand, corresponding to the d → π^* excitation into the

(31) Stratmann, R. E.; Scuseria, G. E.; Frisch, M. J. *J. Chem. Phys.* **1998**, *109*, 8218–8224.
(32) Bauernschmitt, R.; Ahlrichs, R. *Chem. Phys. Lett.* **1996**, *256*, 454–464.
(33) Casida, M. E.; Jamorski, C.; Casida, K. C.; Salahub, D. R. *J. Chem. Phys.* **1998**, *108*, 4439–4449.
(34) Jakubikova, E.; Chen, W.; Dattelbaum, D. M.; Rein, F. N.; Rocha, R. C.; Martin, R. L.; Batista, E. R. *Inorg. Chem.* **2009**, *48*, 10720–10725.
(35) Martin, R. L. *J. Chem. Phys.* **2003**, *118*, 4775–4777.
(36) Turro, N. J. *Modern Molecular Photochemistry*; University Science Books: Herndon, VA, 1991; p 628.
(37) Constable, E. C.; Ward, M. D. *J. Chem. Soc., Dalton Trans.* **1990**, 1405–1409.
(38) Hartshorn, C. M.; Daire, N.; Tondreau, V.; Loeb, B.; Meyer, T. J.; White, P. S. *Inorg. Chem.* **1999**, *38*, 3200–3206.
(39) Barigelletti, F.; Flamigni, L.; Balzani, V.; Collin, J. P.; Sauvage, J. P.; Sour, A.; Constable, E. C.; Cargill Thompson, A. M. W. *Coord. Chem. Rev.* **1994**, *132*, 209–214.
(40) Grosshenny, V.; Ziessel, R. *J. Organomet. Chem.* **1993**, *453*, C19–C22.
(41) Gourdon, A.; Launay, J.-P. *Inorg. Chem.* **1998**, *37*, 5336–5341.
(42) Dose, E. V.; Wilson, L. J. *Inorg. Chem.* **1977**, *17*, 2660–2666.

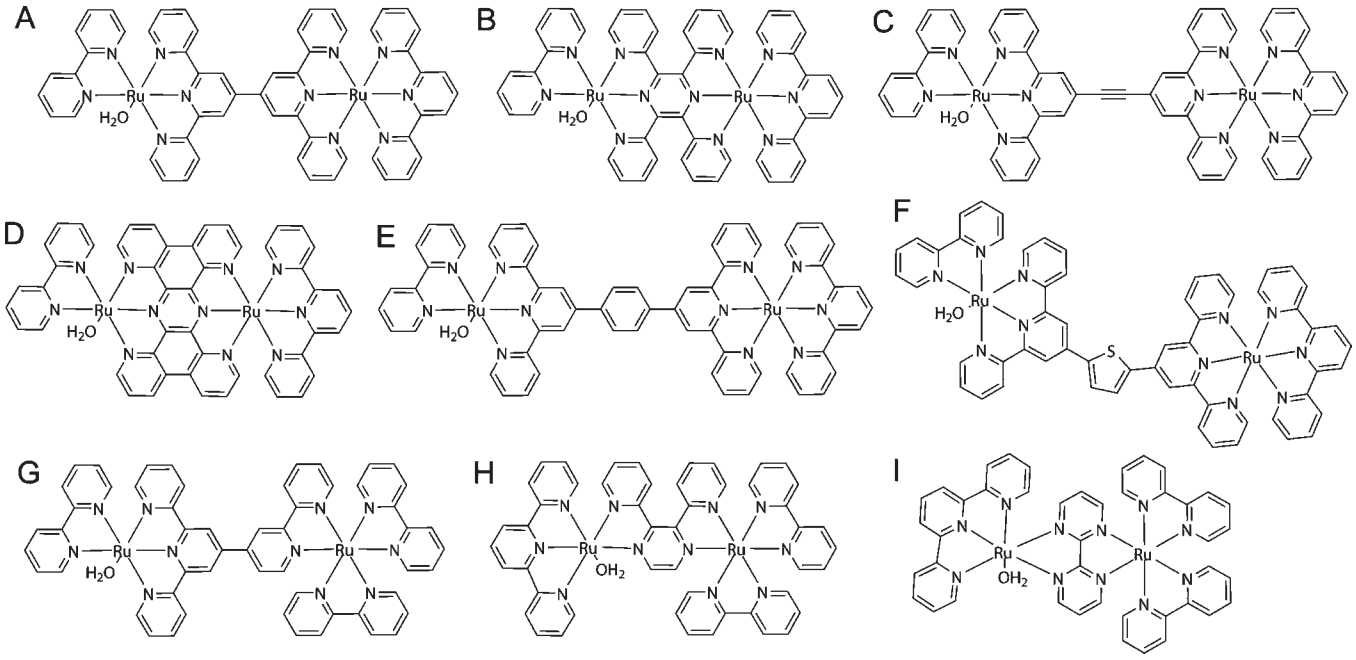

Figure 2. Catalyst−chromophore dyads with different bridging ligands.

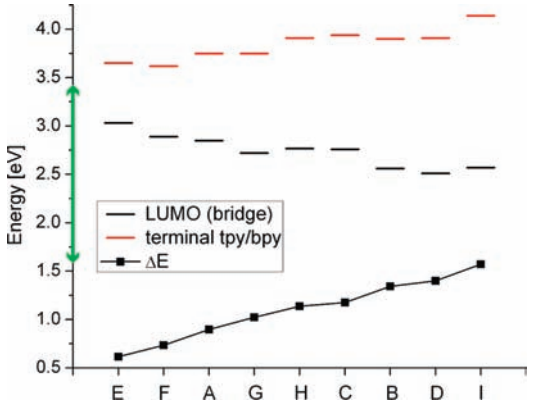

Figure 3. Energy levels of virtual orbitals localized on the bridging ligand and the terminal tpy−bpy ligand of the chromophore. The energies of virtual orbitals are plotted with respect to the energy of the HOMO set at 0 eV. ΔE corresponds to the gap between the two energy levels. Labels A−I correspond to the dimer labels shown in Figure 2. The green interval on the y axis denotes the energy range accessible via excitation by visible light (1.6−3.4 eV) from the HOMO.

bridge. Singly occupied natural orbitals for lowest triplet excited states can be found in the Supporting Information.

In order to gain insight into how the absorption spectrum changes with respect to different bridging ligands, we calculated the absorption spectra in the visible-light region for the selected dimers **A**, **B**, **E**, and **H** (see Figure 4). These dimers were chosen to capture the salient features of all of the different bridging ligands (i.e., correspond to the bridging ligands with various levels of π conjugation). All four dimers display intense absorption peaks at ∼2.45 eV, which correspond to the MLCT transitions into the π^* orbital delocalized over the bridging ligand. Inclusion of the phenylene spacer in the tpy−tpy bridge shifts this peak to ∼2.61 eV because of the partial decoupling of the tpy−tpy π conjugation by the spacer, which results in destabilization of the bridge-localized π^* state (see Figure S8 in the Supporting

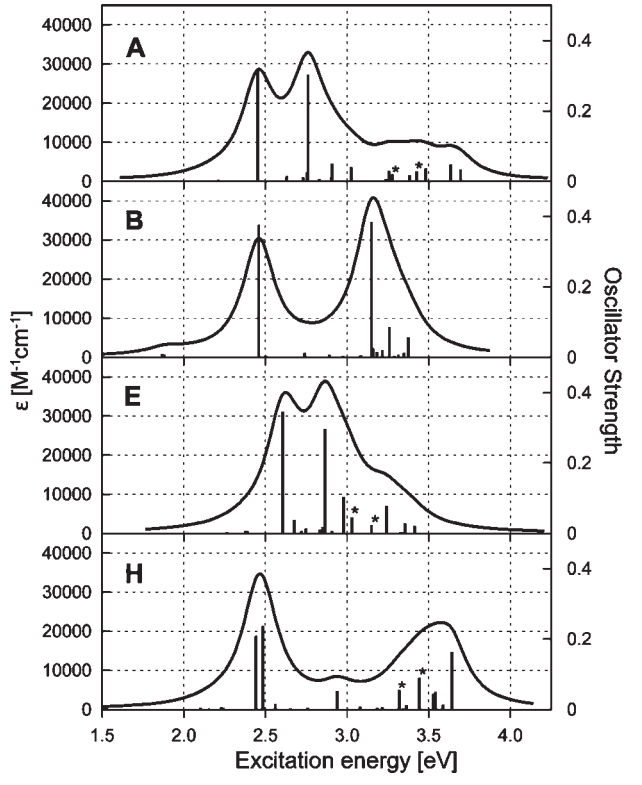

Figure 4. Calculated absorption spectra in vacuo for selected dimers. Stars label excitations in which the electron is mainly localized on the terminal tpy or bpy group and $f > 0.02$.

Information). A second group of MLCT transitions into the bridging ligand is located at 2.76−2.94 eV for dimers **A**, **E**, and **H**. These transitions correspond to excitations into the π^* orbitals located on the bridging tpy group of the chromophore for dimers **A** and **E** and the pyrazine moiety of dimer **H**. The absorption peaks located at 3.15 eV for dimer **B** and 3.6 eV for dimer **H** correspond to the $\pi \rightarrow \pi^*$ transitions centered on the bridging ligands.

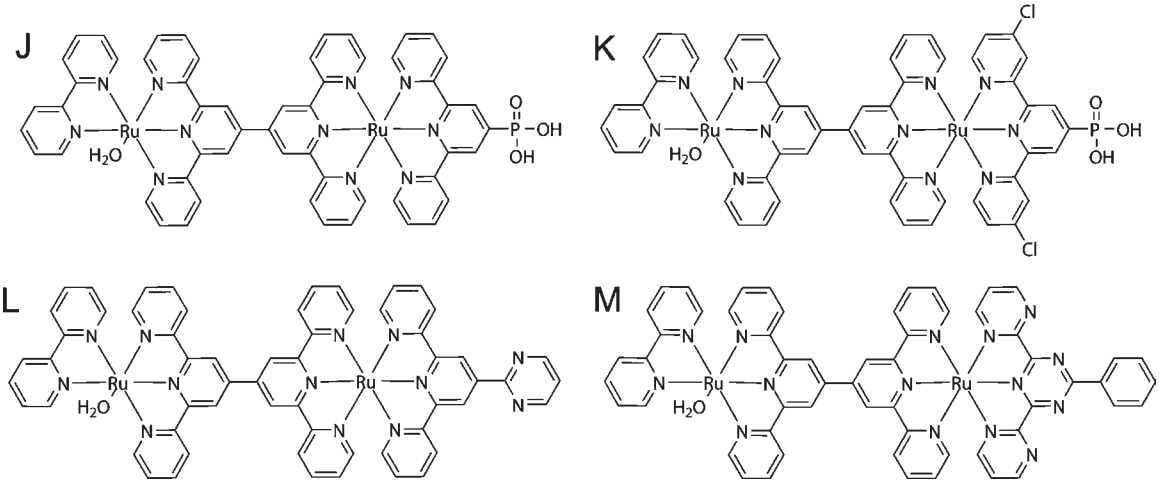

Figure 5. Catalyst−chromophore dyads with a modified terminal tpy group.

Transitions labeled by a star correspond to excitations dominated by a MLCT transition to the terminal tpy or bpy group. As can be seen in Figure 4, these transitions are lower in intensity than the bridge-centered transitions by about an order of magnitude and tend toward the ultraviolet end of the visible spectrum. NTOs corresponding to these excitations are included in the Supporting Information.

Modifications to the Terminal Ligand. Several modifications of the terminal tpy group in the chromophore subunit were studied with the intent of making it more electron-accepting, thereby favoring the spatial localization of the excited electron on the modified terminal ligand rather than on the bridging ligand (see Figure 5). The first modification (**J**) consists of adding phosphonic acid, which is used as a linker for attachment to the metal oxide nanoparticles.[43,44] Other modifications include the attachment of electron-withdrawing groups to the tpy ligand (**K**) and the extension of the π-conjugated system of the tpy ligand (**L** and **M**). These modifications follow from previously reported experimental studies with the aim of increasing the excited-state lifetime of the $[Ru(tpy)_2]^{2+}$ monomer.[45−49] The modified dyads are shown in Figure 5.

A plot showing the energy levels of the lowest-energy virtual orbitals localized on the bridging ligand and the modified terminal tpy ligand, as well as the energy levels of the original dyad (**A**), can be found in Figure 6. A comparison of Figures 3 and 6 shows that the introduction of the phosphonic acid linker (dyad **J**) has virtually no influence on the energy levels of the bridging ligand

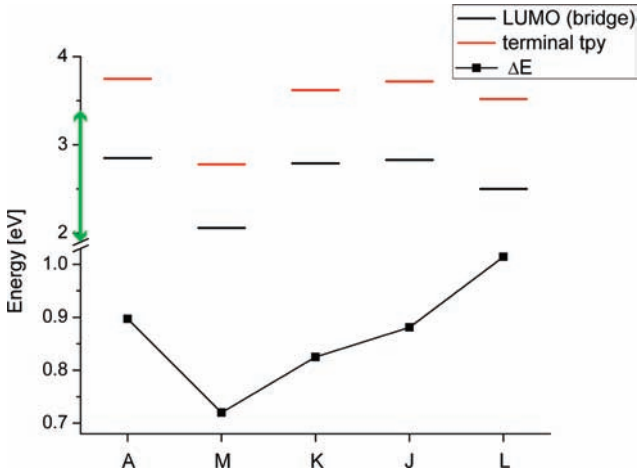

Figure 6. Energy levels of virtual orbitals localized on the bridging ligand and the modified tpy ligand of the chromophore. The energies of virtual orbitals are plotted with respect to the energy of the HOMO set at 0 eV. ΔE corresponds to the gap between the two energy levels. Labels correspond to the dimer labels shown in Figures 2 and 4. The green interval on the *y* axis denotes the energy range accessible via excitation by visible light (1.6−3.4 eV) from the HOMO.

and the terminal tpy ligand. Replacing the tpy ligand by di-2′-pyrimidylphenyl-1,3,5-triazine (dyad **M**) reduces the energy gap from 0.9 to 0.72 eV. Interestingly, the attachment of the pyrimidine ligand to the terminal tpy group (dyad **L**) increases the energy gap to 1.0 eV. In all cases, the LUMO is still localized on the bridging ligand rather than the terminal tpy group and the excited electron in the lowest triplet excited state occupies the π^* orbital located on the bridge as well.

The calculated absorption spectrum for dyad **M** is shown in Figure 7 (in red) along with the spectrum for the unmodified dyad **A** (in black) for comparison. This dyad was chosen because the energy of the virtual orbital localized on the modified tpy ligand is less than 3 eV above the energy of the HOMO (see Figure 6), which indicates the possibility of absorption into this ligand in the visible-light region. Like dyad **A**, dyad **M** displays two strong absorption peaks in the visible-light region. The peak at 2.43 eV corresponds to a MLCT transition into the tpy−tpy bridging ligand, similar to the transitions of the bridge-only-modified dyads. The excitation at 2.43 eV also contains a contribution

(43) Zabri, H.; Gillaizeau, I.; Bignozzi, C. A.; Caramori, S.; Charlot, M.-F.; Cano-Boquera, J.; Odobel, F. *Inorg. Chem.* **2003**, *42*, 6655–6666.
(44) Gillaizeau-Gauthier, I.; Odobel, F.; Alebbi, M.; Argazzi, R.; Costa, E.; Bignozzi, C. A.; Qu, P.; Meyer, G. J. *Inorg. Chem.* **2001**, *40*, 6073–6079.
(45) Schubert, U. S.; Hofmeier, H.; Newkome, G. R. *Modern Terpyridine Chemistry*; Wiley-VCH Verlag GmbH Co. KGaA: Weinheim, Germany, 2006.
(46) Fang, Y.-Q.; Taylor, N. J.; Hanan, G. S.; Loiseau, F.; Passalacqua, R.; Campagna, S.; Nierengarten, H.; Dorsselaer, A. V. *J. Am. Chem. Soc.* **2002**, *124*, 7912–7913.
(47) Fang, Y. Q.; Taylor, N. J.; Laverdiere, F.; Hanan, G. S.; Loiseau, F.; Nastasi, F.; Campagna, S.; Nierengarten, H.; Leize-Wagner, E.; Van Dorsselaer, A. *Inorg. Chem.* **2007**, *46*, 2854–2863.
(48) Polson, M. I. J.; Taylor, N. J.; Hanan, G. S. *Chem. Commun.* **2002**, 1356–1357.
(49) Polson, M. I. J.; Medlycott, E. A.; Hanan, G. S.; Mikelsons, L.; Taylor, N. J.; Watanabe, M.; Tanaka, Y.; Loiseau, F.; Passalacqua, R.; Campagna, S. *Chem.—Eur. J.* **2004**, *10*, 3640–3648.

(~13%) from the d$\pi \rightarrow \pi^*$ transition on the modified terminal ligand, which most likely contributes to the increase in the oscillator strength in comparison to the similar transition for dyad **A** (see the peak at 2.45 eV in Figure 7). The second peak located at 2.83 eV also belongs to a MLCT transition, with the hole localized predominantly on the Ru d orbital and the particle on the bridging tpy group of the modified chromophore. Additionally, the absorption spectrum of dyad **M** contains a d$\pi \rightarrow \pi^*$ transition (at 2.62 eV) and a d $\rightarrow \pi^*$ transition (at 2.97 eV) centered on the modified heteropyridine ligand. NTOs for these transitions are included in the Supporting Information (Figures S11 and S12). Overall, modifications to the terminal tpy group give rise to additional transitions centered at the modified ligand in the visible-light region. The most intense transitions in the visible-light region, however, still belong to d $\rightarrow \pi^*$ transitions into the tpy−tpy bridging ligand.

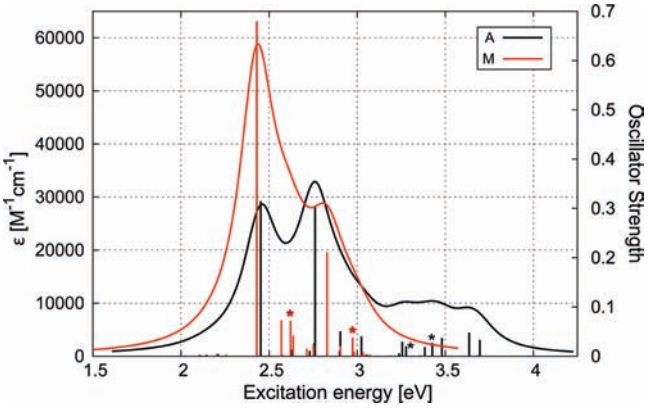

Figure 7. Calculated absorption spectra in vacuo for dyads **M** (in red) and **A** (in black). Stars label excitations in which the electron is mainly localized on the terminal tpy-based group and $f > 0.02$.

In a functional photocatalytic system, the catalyst−chromophore dyad will need to be attached to the TiO_2 nanoparticle by a linker group. Therefore, we investigated the influence of the commonly used phosphonic acid linker on the calculated dyad properties. We compared three dyad pairs that differed only by inclusion of the phosphonic acid linker: dyad **A** with dyad **J** and two dyad pairs based on dyads **L** and **M**. We found that inclusion of the phosphonic acid linker has no significant effect on the character and energy of the LUMO and the lowest-energy virtual orbital located on the terminal ligand. The character of the optimized ^{3}MLCT states also remains unchanged after inclusion of the phosphonic acid linker. We have also calculated the visible absorption spectrum of dyad **M** with the phosphonic acid linker attached and found it to be very similar to the absorption spectrum of dyad **M**. The main difference between the absorption spectra of the two dyads is a group of low-intensity transitions present on dyad **M**−PO_3H_2 involving the p orbitals on the phosphonic acid linker. A more detailed comparison of the molecular orbitals and absorption spectra can be found in the Supporting Information (Figures S15−S17).

Modifications to Both Bridging and Terminal Ligands. Because modification of the bridging ligand or terminal tpy ligand by itself does not achieve our desired objective (i.e., excited electron occupation of the π^* molecular orbital located at the terminal ligand), we design new molecules in which we modify both the bridging and terminal tpy ligands. All modifications are inspired by the bridging and terminal ligands synthesized in the previous experimental studies as described above. In the

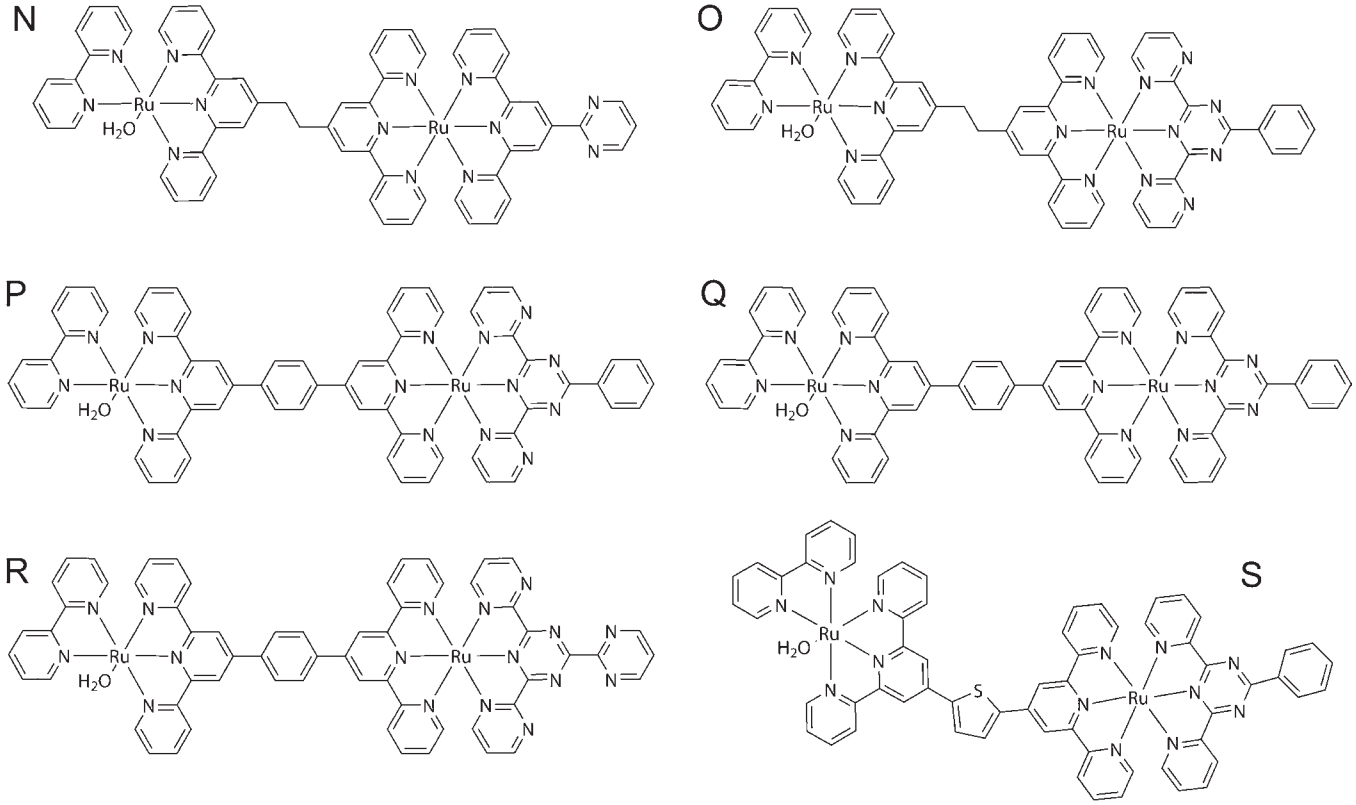

Figure 8. Catalyst−chromophore dyads with modified bridging and terminal tpy groups.

design, the following rules are applied: (1) An additional group (C_2H_4, phenylene, or 2,5-thiophenedyil) is inserted between the tpy groups in the bridging ligand to destabilize the bridge state. (2) The terminal tpy group is replaced by an extended heteroterpyridine ligand to make the terminal ligand more electron-accepting. Dyads considered in this study are shown in Figure 8.

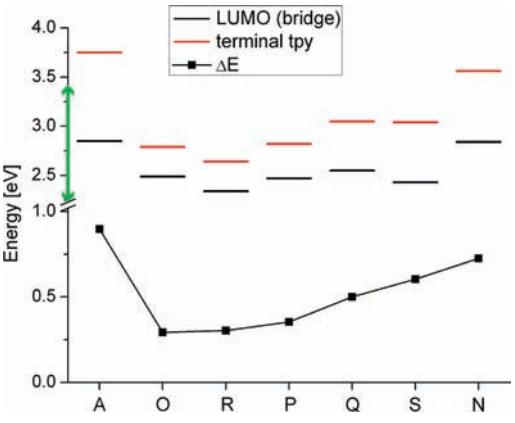

Figure 9. Energy levels of virtual orbitals localized on the bridging ligand and the modified tpy ligand of the chromophore. ΔE corresponds to the gap between the two energy levels. Energies of the virtual orbitals are plotted with respect to the energy of the HOMO set at 0 eV. Labels correspond to the dimer labels shown in Figures 2 and 8. The green interval on the *y* axis denotes the energy range accessible via excitation by visible light (1.6−3.4 eV) from the HOMO.

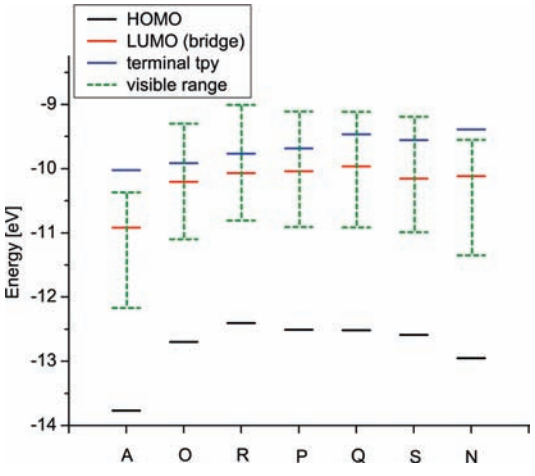

Figure 10. Energy levels of the HOMO and virtual orbitals localized on the bridging ligand and modified terminal tpy ligand of the chromophore. The green lines denote the energy range accessible via excitation by visible light (1.6−3.4 eV) from the HOMO.

Figure 9 displays the virtual orbital energy levels of the lowest-energy orbitals localized on the bridging ligand and the modified terminal tpy ligand. As can be seen from the plot, a combination of both modifications significantly reduces the energy gap between the two orbitals. Moreover, the energy level of the molecular orbital located on the modified terminal tpy ligands for dyads **O**, **P**, **Q**, **R**, and **S** is within the visible-light range (1.6−3.4 eV) from the HOMO. This indicates that the modifications made to these dyads will induce electronic excitations into the π^* orbitals located on terminal ligands upon excitation with visible light. Interestingly, this is achieved by an increase in the energy of the HOMO rather than stabilization of the π^* orbital localized on the terminal ligand (see Figure 10).

The most effective is the combination of tpy−C_2H_4−tpy or tpy−phenylene−tpy bridging ligands with di-2′-pyrimidylphenyl-1,3,5-triazine (**O** and **P**) or 2,4,6-tri-2-pyrimidyl-1,3,5-triazine (**R**). These combinations reduce the energy gap between the π^* orbital on the bridge and the π^* orbital on the terminal ligand to approximately 0.3−0.35 eV. In all cases, the LUMO is still localized on the bridge. The lowest triplet excited state is, however, localized on the modified terminal tpy group for dyads **O**, **P**, and **R** (see Figures 11 and S7 in the Supporting Information). Also, some of the most intense absorption peaks in the visible-light region have a significant contribution from excitation into the modified terminal tpy group (Figure 12). An additional effect of the modifications is a two-fold increase in the absorption intensities of the modified dyads.

The case of the 2,5-thiophenedyil (tpd) spacer (dyads **F** and **S**) is quite interesting. In the ground state, insertion of the tpd spacer between the two tpy groups breaks up the conjugation of the tpy−tpy bridge and decreases the gap between the π^* orbitals localized on the bridge and terminal tpy ligands (see Figure 3). This is due to the presence of two dihedral angles (26−29°) between the tpy groups and the tpd spacer. However, both $[(bpy)(H_2O)Ru(tpy-tpd-tpy)Ru(tpy)]^{4+}$ and $[(bpy)(H_2O)Ru(tpy-tpd-tpy)Ru(adpt)]^{4+}$ (adpt = 2-aryl-4,6-di-2-pyridyl-*s*-triazine) dyads undergo significant structural changes in

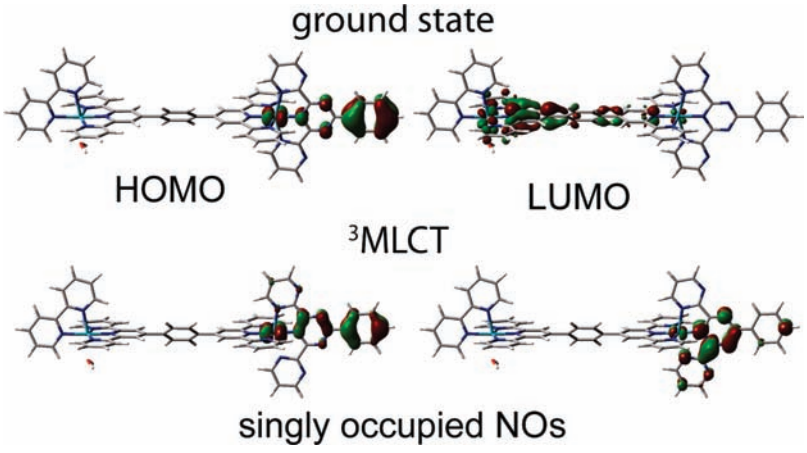

Figure 11. Ground-state frontier molecular orbitals and ^{3}MLCT singly occupied natural orbitals (NOs) for dyad **P**.

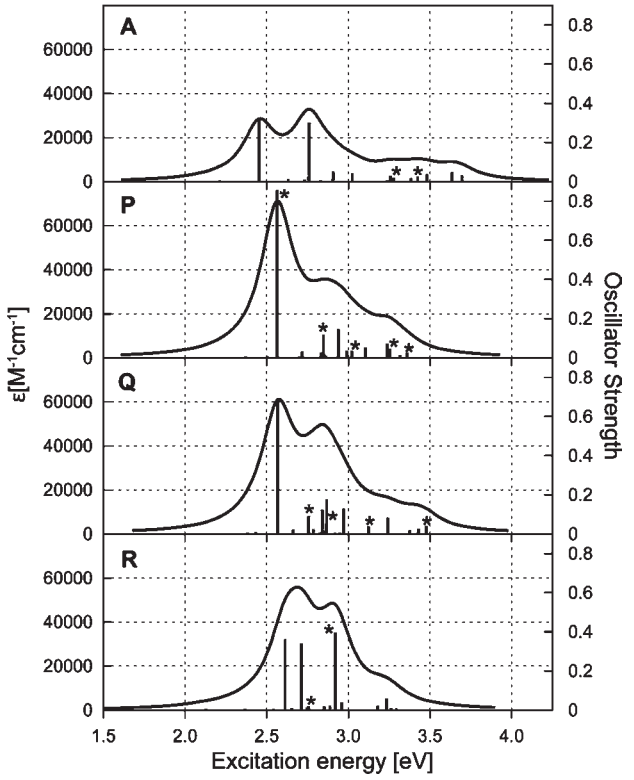

Figure 12. Calculated absorption spectra in vacuo for dimers **P**, **Q**, and **R**. Stars label excitations in which the electron is mainly localized on the modified terminal tpy group and $f > 0.02$. The spectrum of dimer **A** is also shown for comparison.

the excited state, and as a result, the two tpy groups and the tpd spacer become virtually coplanar (the dihedral angles become 1−3°), thus completely extending the π-conjugated system over the tpy−tpd−tpy bridge. Therefore, the lowest ^{3}MLCT state is localized on the bridge rather than the terminal tpy ligand, even after modifications are made to the terminal ligand to make it more electron-accepting. In this respect, the tpd spacer behaves more like an alkyne spacer rather than phenylene or alkane spacers, which break the conjugation between the tpy bridging groups in both ground and excited states.

Finally, we note that there are many other possible modifications of the original catalyst−chromophore dyad (dyad **A**) that might induce (alone or in a combination) the excited electron localization in the terminal ligand attached to the nanoparticle. They include, for example, functionalization of the tpy−tpy bridge by the electron-donating substituents (e.g., methyl groups),[45] introduction of an electron donor, such as tyrosine, between the catalyst and chromophore subunits, mimicking the triad of photosystem II,[50] or cyclometalation of a tpy group.[51] Unfortunately, because of the large number of potential modifications, we were not able to explore all of the possibilities; however, they might be an interesting topic for a future study.

Conclusions

We applied DFT to study a series of catalyst−chromophore dyad assemblies based on the $[(bpy)(H_2O)Ru(tpy-tpy)Ru(tpy)]^{4+}$ dyad (**A**). While dyad **A** absorbs light in the visible-light region, its excited states are localized predominantly on the tpy−tpy bridge and have unfavorable coupling with the conduction band of TiO_2 to promote electron injection. This is due to the fact that the π^*-conjugated system on the bridge is lower in energy (and therefore more electron-accepting) than the π^*-conjugated system on the terminal tpy ligand.

While the addition of a phenylene or an alkane spacer to the tpy−tpy bridging ligand somewhat decouples the bridge-localized π-conjugated system, the modified dyads still absorb visible light mainly into the bridging ligands. Although the 2,5-thiophenedyil spacer seems to decouple the bridge-localized π-conjugated system in the ground state, it actually increases the π conjugation in the excited state by undergoing a structural change, which results in the bridging ligand becoming planar. All additional bridging ligands investigated (tpy−C_2−tpy, tpy−bpy, tetra-2-pyridylpyrazine, tetrapyrido(2,3-*a*:3′,2′-*c*:2″,3″-*h*:3‴,2‴-*j*)phenazine, 2,3-di-2-pyridylpyrazine, and 2,2′-bipyrimidine) increase the π conjugation and thereby the stability of the bridging ligand with respect to the terminal tpy ligand. Overall, we found that the addition of a spacer did not significantly affect the relative stabilities of bridge-localized versus terminal tpy ligand-localized states, leading to a bridge-localized excited electron.

Modifications of the terminal tpy ligand alone by substitution of electron-withdrawing groups (Cl^-) and by extension of the conjugated π system through the addition of a heteroaromatic ring (attachment of the pyrimidine ligand to the terminal tpy group) or replacement of the terminal tpy group by an extended heteropyrimidine ligand (i.e., di-2′-pyrimidylphenyl-1,3,5-triazine) also do not sufficiently stabilize the conjugated π system on the terminal ligand to affect the nature of the excited state.

The most successful modifications, which induce intense electronic excitations into the terminal ligand, include both introduction of the phenylene or alkane spacer into the tpy−tpy bridging ligand and replacement of the terminal tpy ligand by heteropyridine ligands with an extended conjugated π system (di-2′-pyrimidylphenyl-1,3,5-triazine or 2,4,6-tri-2-pyrimidyl-1,3,5-triazine). Dyads with these modifications display both intense absorption into the modified terminal heteropyridine ligand and electron localization on the modified terminal ligand in the lowest ^{3}MLCT state, which should lead to efficient IET upon attachment to the TiO_2 nanoparticle.

Acknowledgment. This work was supported by the Laboratory Directed Research and Development (LDRD) program at Los Alamos National Laboratory. Los Alamos National Laboratory is operated by Los Alamos National Security, LLC, for the National Nuclear Security Administration of the U.S. Department of Energy under Contract DE-AC52-06NA25396.

Supporting Information Available: Absorption spectrum of $[Ru(tpy)_2]^{2+}$ calculated in vacuo and various solvents, plots of the HOMOs and LUMOs localized on the bridge and terminal tpy/bpy ligands and singly occupied natural orbitals for the lowest triplet excited states for all dyads considered in this work, NTOs corresponding to the most intense excitations and excitations centered at the terminal tpy/bpy ligands shown in Figures 4, 7, and 10, comparison of the dyads with and without the phosphonic acid linker, and Cartesian coordinates for optimized ground and excited states. This material is available free of charge via the Internet at http://pubs.acs.org.

(50) Hammarstrom, L.; Sun, L. C.; Akermark, B.; Styring, S. *Catal. Today* **2000**, *58*, 57–69.
(51) Wadman, S. H.; Kroon, J. M.; Bakker, K.; Lutz, M.; Spek, A. L.; van Klink, G. P. M.; van Koten, G. *Chem. Commun.* **2007**, 1907–1909.